Ambient humidity, the overlooked influencer of radioactivity measurements

Pommé, S.; Stroh, H.; Altzitzoglou, T.; Paepen, J.; Van Ammel, R.; Marouli, M.; Verheyen, L.; Unterweger, M.; Fitzgerald, R.; Bergeron, D. E.; Pibida, L.; Nähle, O.; Kossert, K.; Ramirez, N.; Bendall, E.; Fenwick, A.; Ferreira, K.; Keightley, J.; Baker, M.; Collins, S.; Michotte, C.; Courte, S.; Coulon, R.; Jackson, T. W.; Van Wyngaardt, W. M.; Fazio, A.; De Felice, P.; Vodenik, B.; Korun, M.; Juget, F.; Bailat, C.; Nedjadi, Y.; Bochud, F.; Buchillier, T.; Roy, T.; Galea, R.; Kajan, I.; Van Rooy, M. W.; McGinnity, P.; Tucakovic, I.; Osvath, I.; Pelczar, K.

Publisher's version / Version de l'éditeur:
https://doi.org/10.1088/1681-7575/ad0c9f
Metrologia, 61, 1, 2023-11-27

OPEN ACCESS
IOP Publishing | Bureau International des Poids et Mesures Metrologia
Metrologia **61** (2024) 015001 (14pp) https://doi.org/10.1088/1681-7575/ad0c9f

Ambient humidity, the overlooked influencer of radioactivity measurements

S Pommé[1,*], H Stroh[1], T Altzitzoglou[1], J Paepen[1], R Van Ammel[1], M Marouli[1], L Verheyen[2], M Unterweger[3], R Fitzgerald[3], D E Bergeron[3], L Pibida[3], O Nähle[4], K Kossert[4], N Ramirez[5], E Bendall[5], A Fenwick[5], K Ferreira[5], J Keightley[5], M Baker[5], S Collins[5], C Michotte[6], S Courte[6], R Coulon[6], T W Jackson[7], W M Van Wyngaardt[7], A Fazio[8], P De Felice[8], B Vodenik[9], M Korun[9], F Juget[10], C Bailat[10], Y Nedjadi[10], F Bochud[10], T Buchillier[10], T Roy[11], R Galea[11], I Kajan[12], M W Van Rooy[13], P McGinnity[14], I Tucakovic[14], I Osvath[14] and K Pelczar[1]

[1] European Commission, Joint Research Centre (JRC), Geel, Belgium
[2] Belgian Nuclear Research Centre (SCK CEN), Mol, Belgium
[3] Physical Measurement Laboratory, National Institute of Standards and Technology (NIST), Gaithersburg, MD, United States of America
[4] Physikalisch-Technische Bundesanstalt (PTB), Braunschweig, Germany
[5] National Physical Laboratory (NPL), Teddington, United Kingdom
[6] Bureau International des Poids et Mesures (BIPM), Sèvres, France
[7] Australian Nuclear Science and Technology Organisation (ANSTO), Lucas Heights, Australia
[8] National Institute of Ionizing Radiation Metrology (ENEA), Casaccia Research Centre, Roma, Italy
[9] Jožef Stefan Institute (JSI), Ljubljana, Slovenia
[10] Institut de Radiophysique, Lausanne (IRA), Switzerland
[11] National Research Council of Canada (NRC), Ottawa, Canada
[12] Paul Scherrer Institute (PSI), Villigen, Switzerland
[13] Radioactivity Standards Laboratory (NMISA), Cape Town, South Africa
[14] International Atomic Energy Agency—Marine Environment Laboratories (IAEA), Monaco, Monaco

E-mail: stefaan.pomme@ec.europa.eu

Received 6 September 2023, revised 13 November 2023
Accepted for publication 14 November 2023
Published 27 November 2023

Abstract

When verifying the validity of the exponential-decay law through 137 precise decay rate measurement series at various nuclear laboratories, minor violations have been observed in the shape of annual cycles in the residuals with different amplitudes and phase shifts. The timing and amplitude of these deviations have been compared with local weather data and it appears that ambient humidity is highly correlated with the observed instabilities in these radioactivity measurements. In fact, when compensating the residuals for a linear relationship with absolute humidity in air, most of the annual cycles are no longer statistically significant. As a result, the validity of the exponential-decay law can now be demonstrated with even higher fidelity.

Keywords: exponential-decay law, radioactivity, humidity, solar neutrino, dark matter

* Author to whom any correspondence should be addressed.

1. Introduction

Science-based decision making crucially depends on the quality of the metrology from which it derives its information [1, 2]. Measurements with incomplete uncertainty budgets can lead to misinterpretations of the phenomena under investigation, possibly with fundamental implications in science and policy making [3]. One of the most persistent misunderstandings concerning radionuclide metrology is the assertion that cyclic variations in measured decay rates are caused by space weather phenomena, in particular by neutrinos emitted from the Sun or dark matter [4]. Some authors are adamant in their claims that observed violations of the exponential-decay law cannot be attributed to environmental conditions in the laboratory [5, 6]. However, using historical weather data available on meteorological websites, a link with terrestrial weather could be established for several infamous experiments [1, 2, 4, 7–19].

The most obvious weather attribute suspected of influencing activity measurements would be temperature, hence the common practice to stabilise the room temperature in nuclear laboratories by circulation of heated or cooled air. The air conditioning system may also affect the air humidity in the room, however not every system is set up to keep the absolute humidity stable. The ambient air humidity outside the building easily enters the ventilated rooms of the laboratory and affects the behaviour of detectors and their electronics as well as the circulation of radon and travel paths of radioactive particles in air. It may be true that ambient humidity is an often overlooked culprit of instability in activity measurements. One could argue that its effects are generally insignificant in the uncertainty budget of absolute activity measurements. Few metrologists will consider small humidity-induced effects in the context of e.g. alpha spectrometry [20] or routine gamma-ray spectrometry [21], considering that the measurement uncertainty typically ranges from 2% to 30%. It is even seldom taken into account in primary standardisation methods for activity [22–28], where uncertainties can go down to 0.1% or even lower [29–31].

Nevertheless, there are circumstances in which the impact of tiny instabilities in activity measurements gains significance. This applies mainly to precise relative measurements, and in particular to half-life measurement series, which can be interpreted as a chain of relative activity measurements over time [32]. The repeatability requirement of half-life experiments exceeds that of absolute measurements by one or more orders of magnitude. For example, better than 0.02% medium-term stability was demonstrated in alpha decay with planar Si detectors [33, 34] and repeatability in an ionisation chamber (IC) is of the order of 0.04% [35]. That explains why half-life measurements are a magnifying glass for underlying metrological imperfections and why their uncertainties have often been underestimated in the literature [32, 36–38]. Not controlling such sources of error and their propagation gives room to alternative interpretations of an experiment. Therefore, when annual cycles in activity measurement series are observed [39], it is incumbent upon the metrological community to provide an explanation and to take corrective action.

In former work, some of the most precise and extensive activity measurement series from laboratories across the world were analysed to investigate the hypotheses that solar neutrinos induce annual and monthly cycles in decay due to variations in Earth–Sun distance [7–10] and internal solar dynamics [12], respectively. Contrary to the monthly cycles, some of the annual cycles were statistically significant, but they were not aligned in phase or amplitude. On this basis, the 'solar neutrino-induced decay' hypothesis could be rejected. In this work, ambient humidity is investigated as a plausible culprit for the occurrence of the annual cycles. Using historical weather data from nearby stations, a linear relationship is established between ambient humidity (or dew point) and residuals from exponential decay. The amplitudes of the annual cycles are redetermined after compensating the residuals for this hypothetical humidity effect. If the magnitudes of the cycles can be reduced below statistically significant levels, the hypothesis gains credibility, and the validity of the exponential-decay law can be confirmed with higher fidelity.

2. Analysis of decay rate series at JRC

2.1. Ambient humidity

Data from a temperature (T) and relative humidity (H_r) monitor inside the radionuclide metrology laboratory 35 A in building 010 of the JRC in Geel were extracted to calculate the absolute humidity (H_a) through the ideal gas equation [40]

$$H_a[\mathrm{g\,m^{-3}}] = \frac{2.1674\,P_s[\mathrm{hPa}]\,H_r[\%]}{273.15 + T[^\circ\mathrm{C}]} \tag{1}$$

in which the quantities must be expressed in the indicated units, and P_s represents a heuristic formula for the saturation vapour pressure above water as a function of temperature [41]

$$P_s[\mathrm{hPa}] = 6.112\exp\left(\frac{17.67\,T[^\circ\mathrm{C}]}{243.5 + T[^\circ\mathrm{C}]}\right). \tag{2}$$

The equation (2) is considered accurate enough (≈0.1% for T between −30 °C and +35 °C) without applying an enhancement factor (for moist air compared to pure water vapour, as a function of atmospheric pressure) or a different approximation below 0 °C [42, 43].

Starting from the relationship $H_r/100 = P_s(T_D)/P_s(T)$, the dew point T_D can be derived from the measured temperature and relative humidity through [44]

$$T_D\,[^\circ\mathrm{C}] = \frac{243.5\,X(H_r,T)}{17.67 - X(H_r,T)} \tag{3}$$

with

$$X(H_r,T) = \left(\ln\left(\frac{H_r[\%]}{100}\right) + \frac{17.67\,T[^\circ\mathrm{C}]}{243.5 + T[^\circ\mathrm{C}]}\right). \tag{4}$$

These data measured inside the laboratory in Geel will be compared with external data from a weather station [45] in the Antwerp airport, located about 43 km away.

The JRC laboratories use an air circulation system that establishes underpressure in certain containment areas and regulates the temperature typically within (21 ± 1) °C. However, there have been some variations in the system's settings over the years, as well as exceptional periods where the system (or sensors) did not function adequately. Figure 1(a) displays the relationship between inside and outside daily average temperatures over the past decade. The inside temperature remains relatively stable during colder days, but there is a slight positive quadratic trend overall. Despite the strong correlation between activity measurements in the ionisation chamber IC1 [1, 2, 46, 47] and outside temperature, they are only weakly correlated with the inside temperature. Therefore, the inside temperature is not the main driving force behind IC1's seasonal effect, and air humidity in the room is more likely the culprit.

Figures 1(b) and (c) show the relationships between inside and outside absolute humidity and dew point, respectively. There is a linear relationship between the humidity data, except at the most humid days (outside $H_a > 10.3$ g m^{-3}) when the inside humidity is visibly flattened by the air-conditioning system. A similar plot is obtained for inside versus outside dew point, since part of the humidity in the incoming air condensates as soon as the dew point exceeds the temperature of the cooling element. The mechanism is more pertinently visible in figure 1(d), which depicts the deviation of the inside humidity H_a from a linear relationship with outside humidity H_a as a function of the outside dew point T_D. The graphs also indicate that weather data collected tens of kilometres away are representative of the external conditions surrounding the laboratory.

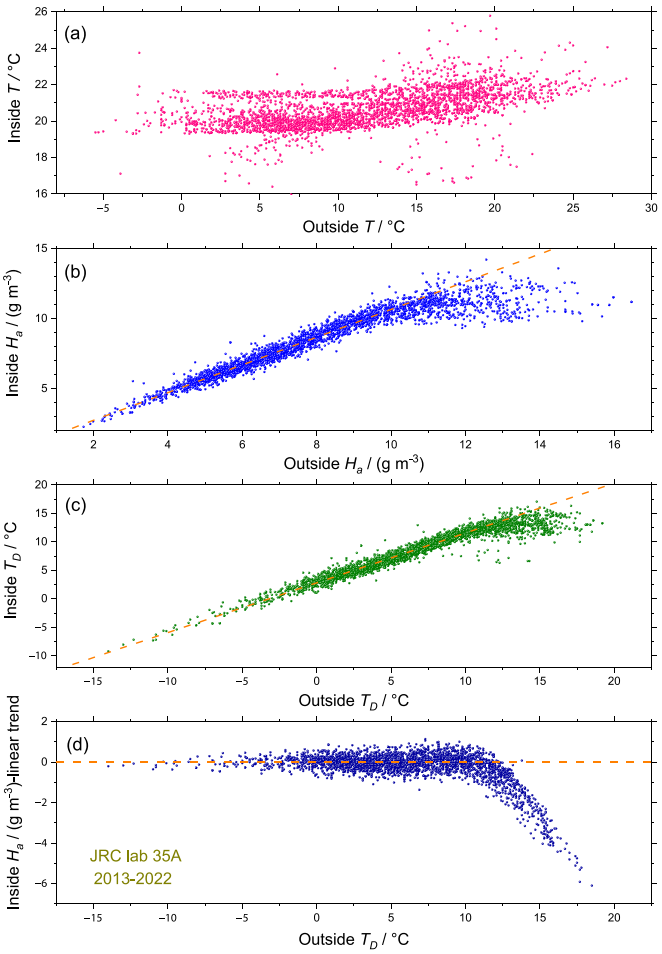

Figure 1. Relationship between (a) inside vs outside daily average temperature, (b) inside vs outside absolute humidity with linear trendline, (c) inside vs outside dew point, (d) deviation of inside humidity from the trendline as a function of outside dew point. The data were collected over the period 2013–2022 in laboratory 35 A, where the ionisation chamber IC1 is located, and compared with matching data from the weather station in the airport of Antwerp. (In figures (b) and (d), a small fraction of deviant data were filtered to enhance the most common trend.).

2.2. ^{22}Na and ^{134}Cs in IC1

The decay curves of a single ^{22}Na source [46] and two ^{134}Cs sources [47] have been regularly monitored in the ionisation chamber IC1 from 2010 to 2022. The residuals of the measured activity rates to an exponential decay function exhibit a high negative correlation ($\rho = -0.55$ and $\rho = -0.59$) with the absolute ambient humidity. Figure 2 shows the averaged residuals of the two ^{134}Cs sources binned by corresponding absolute humidity values outside the laboratory, with a bin width of 0.2 g m^{-3}. There is a clear downward linear trend of the residuals between 3 g m^{-3} and 11 g m^{-3}, which appears to break at higher humidity levels. This can be attributed to the drying effect of the laboratory's air-conditioning system. A similar trendline has been observed in the ^{22}Na data [46].

The ambient humidity undergoes a seasonal cycle that follows the average ambient temperature, as heat drives evaporation of water and increases the humidity capacity of air. Due to their sensitivity to humidity, the ^{22}Na and ^{134}Cs activity measurements in IC1 exhibit an annual cycle with an amplitude of 0.0055% and a phase shift of 50 d. Figure 3 confirms that this cycle is well synchronised with ambient humidity, and less so with the Earth–Sun distance (as seen in the variation in solar neutrino flux) or local temperature.

2.3. Power of annual cycle

The amplitude A of the annual cycle in the residuals from exponential decay is determined from a weighted fit of a sinusoidal

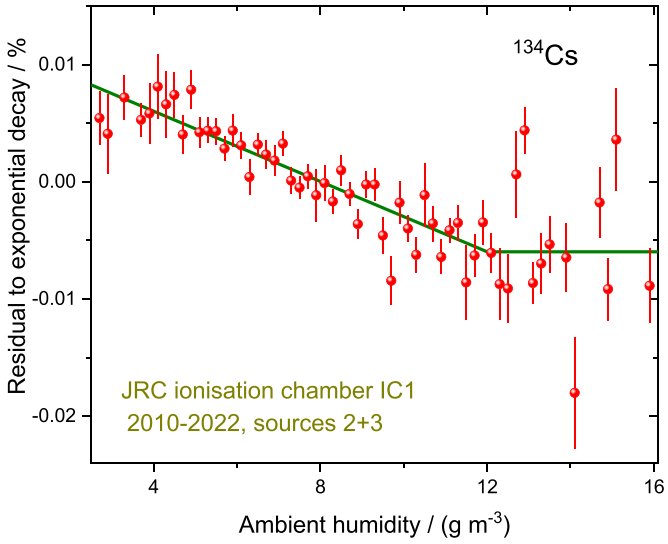

Figure 2. Average values and standard uncertainty of residuals to exponential decay of ^{134}Cs in JRC's ionisation chamber IC1 in Geel, binned as a function of ambient humidity obtained from a weather station in Antwerp.

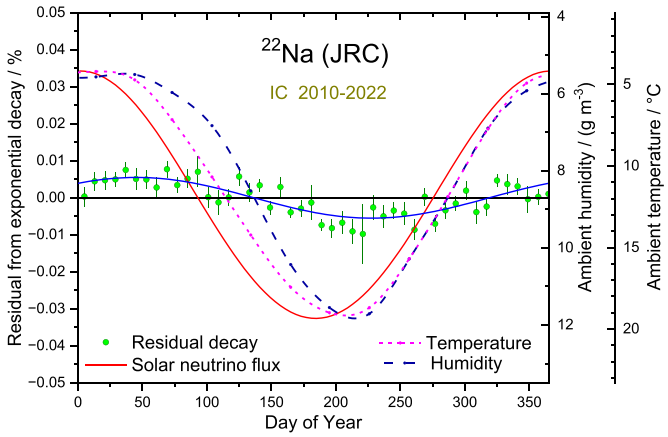

Figure 3. Average residuals from exponential decay for ^{22}Na decay rates measured in IC1, binned over fixed periods in the year, and a fitted sinusoidal cycle through the data. The lines represent the expected relative change in solar neutrino flux hitting Earth (full line), the average ambient temperature (short dash) and humidity (long dash).

function $f(x) = Ax$, in which $x = \sin((t + a)/365)$, t is the day of the year, and a the phase shift. To account for uneven distributions of x, the amplitude is normalised to $A' = A\sqrt{2s_x^2}$. The statistical uncertainty on A' (when generated by normally distributed noise) is easily calculated from the uncertainty of the weighted mean of the residuals, $\sigma_{A'}^2 = 2\sigma_{y_w}^2$ [48]. The ratio $k = A'/\sigma_{A'}$ determines the power $S = k^2/2$ and the probability $P = \mathrm{e}^{-S}$ that a power above S may be produced from random noise.

The method used in previous work [7–10] differs slightly as the data were binned in time zones and the uncertainty of the amplitude was derived by changing its value until the chi-squared (χ^2) of the fit varied by unity. In this work, the power of the annual cycle in decay series will be compared before and after compensation for a humidity effect. For example, the power of the ^{134}Cs and ^{22}Na cycles dropped from 124 and 54 to statistically acceptable levels of 3.8 and 2.9, respectively.

2.4. Other nuclides

Other nuclides, including ^{54}Mn, ^{65}Zn, ^{177}Lu, ^{109}Cd, ^{124}Sb, and ^{226}Ra, have been measured in the same IC [49–53]. Although these data sets are less elaborate, they also exhibit a humidity effect. Extensive decay rate series of two ^{209}Po sources measured with Si detectors show no significant correlation with humidity [34, 35]. The same conclusion applies to repeated activity measurements of ^{3}H and ^{14}C in a liquid scintillation detector (LSC) [9], ^{55}Fe in an x-ray counter with defined solid angle using a gas counter [54] and a large pressurised gas proportional counter [55], as well as a combination of ^{230}U decay rates taken with a CsI sandwich spectrometer, LSC, pressurised proportional counter, and planar Si detectors [56]. The findings are summarised in table 1.

3. Measurements at other metrology institutes

3.1. Procedure

Additional evidence has been collected from metrology institutes in various locations. The obtained decay rate series were optimised to detect annual cycles by removing outlying data points and compensating apparent discontinuities or systematic trends with time using linear functions covering relatively large time periods. Weather data were collected from nearby weather stations (Weather Underground, 2023) and a linear regression analysis was conducted to establish a linear relationship $e_A \propto a + bH_\mathrm{a}$ between the absolute ambient humidity, H_a, and the residuals from exponential decay, e_A. Activity data without corresponding humidity measurements were excluded from analysis. The amplitude and power of annual cycles in activity series were determined before and after compensation for the hypothesised humidity effect ($e_A \leftrightarrow e_A - a - bH_\mathrm{a}$), and the results are summarised in table 1.

3.2. NIST

The NIST has provided historical decay measurements of various nuclides, including ^{22}Na, ^{60}Co, ^{82}Sr, ^{109}Cd, ^{133}Ba, ^{137}Cs, ^{152}Eu, ^{207}Bi, ^{228}Th, and ^{226}Ra, obtained with ICs [57, 58]. Additionally, a decay series of ^{60}Co was measured by coincidence counting, ^{3}H by internal gas counting, and ^{82}Sr by γ-ray spectrometry with a HPGe detector. Humidity data were extracted from the weather station at the Washington Dulles Airport (Sterling). To suppress the influence of instabilities on the measurements obtained from the 'IC A' chamber, the source current was taken relative to that of a ^{226}Ra reference source. As a result, a mild annual cycle was observed in the measurements, which was reduced after compensation for the hypothesised humidity effect.

Table 1. Characteristics of the decay rate measurement sets analysed: (i) decay mode, (ii) radionuclide, (iii) institute at which the measurement series was performed, (iv) method acronym (explained below the table[a]), (v) period indicating the first and last year in which data were collected, (vi) number of data included in the analysis, (vii) normalised amplitude and standard uncertainty of the annual cycle in the residuals of the raw data to a purely exponential decay, (viii) matching power of the cycle, (ix) normalised amplitude and standard uncertainty of the annual cycle in the residuals of the data that have been compensated for a linear dependency on absolute ambient humidity, (x) matching power of the cycle. The order of magnitude of the standard uncertainty on the amplitude, indicated between parentheses, corresponds to that of the last digit of the value of A'.

						Raw data		Humidity-compensated	
Decay mode(s)	Nuclide	Institute	Method	Period/year	#Data	Amplitude A'/%	Power S	Amplitude A'/%	Power S
β^-	^{3}H	JRC	LSC	2002–2014	706	0.052 (22)	2.7	0.035 (22)	1.2
β^-	^{3}H	NIST	IGC	1963–1999	17	0.22 (28)	0.3	0.21 (28)	0.3
β^-	^{14}C	JRC	LSC	2002–2014	706	0.012 (15)	0.3	0.009 (15)	0.2
β^-	^{14}C	NMISA	TDCR	1994–2014	32	0.05 (9)	0.1	0.05 (9)	0.1
β^-, EC	^{36}Cl	PTB	LSC	2009–2013	66	0.0041 (16)	3.2	0.0032 (16)	1.9
β^-	^{60}Co	NIST	IC	1973–2007	198	0.001 (9)	0.0	0.010 (9)	0.7
β^-	^{60}Co	NIST	LTAC	2006–2014	26	0.013 (15)	0.4	0.014 (15)	0.4
β^-	^{60}Co	PTB	IC K	2016–2020	649	0.0138 (12)	64	0.0036 (12)	4.4
β^-	^{60}Co	PTB	IC U	2019–2022	471	0.0042 (18)	2.6	0.0021 (18)	0.7
β^-	^{60}Co	JSI	HPGe	1998–2016	14 942	0.018 (16)	0.6	0.018 (16)	0.6
β^-	^{60}Co	IAEA	HPGe #12	2018–2023	121	0.19 (10)	1.7	0.18 (10)	1.5
β^-	^{60}Co	IAEA	HPGe #15	2018–2023	149	0.33 (13)	3.4	0.18 (13)	1.0
β^-	^{60}Co	IAEA	HPGe 100	2018–2022	169	0.09 (9)	0.5	0.07 (9)	0.3
β^-	^{60}Co	IAEA	HPGe 170	2018–2022	123	0.33 (14)	2.8	0.33 (14)	2.8
β^-	^{85}Kr	PTB	IC K	1999–2020	2432	0.0020 (20)	0.5	0.0010 (20)	0.1
β^-	^{85}Kr	PTB	IC U	2019–2022	379	0.008 (5)	1.4	0.002 (5)	0.1
β^-	^{90}Sr	PTB	IC K	1999–2016	1986	0.023 (2)	52	0.012 (2)	15
β^-	^{90}Sr	PTB	TDCR	2013–2014	4493	0.0036 (14)	3.5	0.0036 (14)	3.6
β^-	^{124}Sb	JRC	IC	2007	55	0.0032 (21)	1.2	0.0031 (21)	1.1
β^-	^{124}Sb	PTB	IC K	2007–2008	232	0.007 (5)	0.8	0.001 (5)	0.0
β^-	^{134}Cs	JRC	IC	2010–2022	1268	0.0051 (3)	124	0.0009 (3)	3.8
β^-	^{137}Cs	PTB	IC K	1999–2020	2149	0.0013 (9)	1.0	0.0007 (9)	0.2
β^-	^{137}Cs	PTB	IC U	2019–2022	415	0.0083 (22)	7.4	0.0066 (22)	4.7
β^-	^{137}Cs	NIST	IC	1973–2007	229	0.004 (9)	0.1	0.004 (9)	0.1
β^-	^{137}Cs	IRA	IC	1997–2012	135	0.014 (10)	0.9	0.007 (10)	0.2
β^-	^{137}Cs	NRC	IC #1-3	1995–2009	51	0.030 (15)	2.0	0.005 (15)	0.1
β^-	^{137}Cs	IAEA	HPGe #12	2018–2023	120	0.05 (9)	0.2	0.05 (9)	0.2
β^-	^{137}Cs	IAEA	HPGe #15	2018–2023	146	0.18 (10)	1.7	0.14 (10)	1.0
β^-	^{137}Cs	IAEA	HPGe 100	2018–2022	168	0.16 (9)	1.6	0.12 (9)	0.9
β^-	^{137}Cs	IAEA	HPGe 170	2018–2022	127	0.23 (13)	1.7	0.07 (13)	0.2
β^+, EC	^{22}Na	JRC	IC	2007–2022	524	0.0054 (5)	54	0.0013 (5)	2.9
β^+, EC	^{22}Na	NIST	IC	1968–1982	87	0.018 (13)	0.9	0.012 (13)	0.4
EC	^{54}Mn	JRC	IC	2006–2009	156	0.0047 (11)	9.5	0.0026 (11)	2.7
EC	^{54}Mn	PTB	IC	2010–2016	716	0.014 (3)	12	0.004 (3)	1.3
EC	^{55}Fe	JRC	PC	2004–2005	595	0.0044 (17)	3.4	0.0030 (17)	1.6
EC	^{55}Fe	JRC	PPC	2001–2018	47	0.005 (8)	0.2	0.003 (8)	0.1
EC	^{57}Co	NIST	IC	1962–1966	73	0.060 (24)	3.2	0.058 (24)	3.0
EC, β^+	^{65}Zn	JRC	IC	2002–2003	92	0.007 (6)	0.7	0.011 (6)	1.7
EC(,β^+)	^{82}Sr/^{82}Rb + ^{85}Sr	NIST	IC	2007–2008	158	0.0006 (25)	0.0	0.0018 (25)	0.3
EC(,β^+)	^{82}Sr/^{82}Rb	NIST	HPGe	2007–2008	25	0.11 (13)	0.4	0.07 (13)	0.2
EC, IT	^{108m}Ag	PTB	IC K	1999–2020	2361	0.0196 (16)	80	0.0043 (16)	3.8
EC, IT	^{108m}Ag	PTB	IC U	2019–2022	411	0.007 (4)	1.7	0.003 (4)	0.3
EC	^{109}Cd	JRC	IC	2006–2010	123	0.0111 (21)	13	0.0071 (21)	5.4
EC	^{109}Cd	NIST	IC	1976–1981	167	0.013 (12)	0.6	0.008 (12)	0.2
EC	^{109}Cd	JSI	HPGe	1998–2016	5311	0.052 (36)	1.1	0.050 (36)	1.0
EC	^{133}Ba	NIST	IC	1979–2012	130	0.030 (6)	12	0.011 (6)	1.5
EC	^{133}Ba	PTB	IC K	1999–2020	2437	0.004 (5)	0.4	0.004 (5)	0.4
EC	^{133}Ba	PTB	IC U	2019–2022	417	0.020 (11)	1.8	0.009 (11)	0.4

(Continued.)

Table 1. (Continued.)

Decay mode(s)	Nuclide	Institute	Method	Period/year	#Data	Raw data		Humidity-compensated	
						Amplitude A'/%	Power S	Amplitude A'/%	Power S
EC, β^-, β^+	^{152}Eu	NIST	IC	1976–2011	96	0.024 (9)	4.0	0.017 (9)	2.1
EC, β^-, β^+	^{152}Eu	PTB	IC K	1999–2020	2367	0.0072 (13)	16	0.0016 (13)	0.8
EC, β^-, β^+	^{152}Eu	PTB	IC U	2019–2022	421	0.014 (5)	4.3	0.014 (5)	4.4
EC, β^-, β^+	^{152}Eu	NPL	HPGe	2017–2023	265	0.28 (9)	5.3	0.11 (9)	1.4
EC, β^-, β^+	^{152}Eu	SCK	HPGe #8	2008–2017	3 × 498	0.057 (27)	2.3	0.051 (27)	1.8
EC, β^-, β^+	^{152}Eu	SCK	HPGe #10	2008–2016	3 × 470	0.075 (18)	8.4	0.049 (18)	3.7
EC, β^-, β^+	^{152}Eu	SCK	HPGe #11	2008–2017	3 × 501	0.071 (22)	5.2	0.058 (22)	3.4
EC, β^-, β^+	^{152}Eu	SCK	HPGe #13	2008–2017	3 × 519	0.163 (25)	21	0.052 (25)	2.3
EC, β^-, β^+	^{152}Eu	SCK	HPGe #16	2008–2016	3 × 452	0.066 (16)	8.9	0.058 (16)	7.0
EC, β^-, β^+	^{152}Eu	SCK	HPGe #17	2014–2017	3 × 186	0.043 (22)	1.8	0.039 (22)	1.5
EC, β^-, β^+	^{152}Eu	SCK	HPGe #20	2013–2019	3 × 332	0.005 (31)	0.0	0.015 (31)	0.1
EC, β^-, β^+	^{152}Eu	SCK	HPGe #21	2008–2017	3 × 419	0.018 (24)	0.0	0.019 (24)	0.1
EC, β^-, β^+	^{152}Eu	SCK	HPGe #23	2011–2017	3 × 282	0.089 (35)	3.2	0.067 (35)	1.8
EC, β^-, β^+	^{152}Eu	SCK	HPGe #24	2011–2017	3 × 308	0.017 (16)	0.6	0.016 (16)	0.5
EC, β^-, β^+	^{152}Eu	SCK	HPGe #25	2011–2017	3 × 325	0.017 (16)	6.2	0.016 (16)	2.3
EC, β^-, β^+	^{152}Eu	SCK	HPGe #26	2013–2017	3 × 248	0.030 (24)	0.8	0.018 (24)	0.3
EC, β^-, β^+	^{152}Eu	SCK	HPGe #27	2011–2017	3 × 304	0.070 (31)	0.8	0.019 (31)	0.3
EC, β^-, β^+	^{152}Eu	SCK	HPGe #28	2014–2017	3 × 187	0.036 (22)	1.4	0.033 (22)	1.2
EC, β^-, β^+	^{152}Eu	SCK	HPGe #8	2019–2022	3 × 199	0.146 (42)	6.2	0.147 (42)	6.2
EC, β^-, β^+	^{152}Eu	SCK	HPGe #9	2020–2022	3 × 137	0.059 (29)	2.0	0.019 (29)	0.2
EC, β^-, β^+	^{152}Eu	SCK	HPGe #10	2019–2022	3 × 217	0.082 (34)	2.9	0.083 (34)	2.9
EC, β^-, β^+	^{152}Eu	SCK	HPGe #11	2020–2022	3 × 129	0.059 (45)	0.9	0.067 (45)	1.1
EC, β^-, β^+	^{152}Eu	SCK	HPGe #13	2019–2022	3 × 214	0.031 (36)	0.4	0.033 (36)	0.4
EC, β^-, β^+	^{152}Eu	SCK	HPGe #14	2019–2022	3 × 191	0.090 (29)	5.0	0.094 (29)	5.3
EC, β^-, β^+	^{152}Eu	SCK	HPGe #19	2019–2022	3 × 197	0.061 (28)	2.5	0.060 (28)	2.4
EC, β^-, β^+	^{152}Eu	SCK	HPGe #21	2019–2022	3 × 182	0.094 (50)	1.8	0.077 (50)	1.2
EC, β^-, β^+	^{152}Eu	SCK	HPGe #22	2020–2022	3 × 87	0.029 (35)	0.8	0.008 (35)	0.0
EC, β^-, β^+	^{152}Eu	SCK	HPGe #23	2019–2020	3 × 58	0.059 (53)	0.6	0.065 (53)	0.8
EC, β^-, β^+	^{152}Eu	SCK	HPGe #24	2021–2022	3 × 91	0.035 (34)	0.5	0.020 (34)	0.2
EC, β^-, β^+	^{152}Eu	SCK	HPGe #25	2019–2022	3 × 168	0.056 (23)	2.9	0.023 (23)	0.5
EC, β^-, β^+	^{152}Eu	SCK	HPGe #26	2019–2022	3 × 193	0.099 (39)	3.2	0.052 (39)	0.9
EC, β^-, β^+	^{152}Eu	SCK	HPGe #27	2019–2022	3 × 194	0.106 (39)	3.8	0.097 (39)	3.2
EC, β^-, β^+	^{152}Eu	SCK	HPGe #28	2019–2022	3 × 194	0.048 (29)	1.4	0.041 (29)	1.0
EC, β^-, β^+	^{152}Eu	SCK	HPGe #30	2019–2022	3 × 155	0.040 (23)	1.6	0.022 (23)	0.5
EC, β^-, β^+	^{152}Eu	SCK	HPGe #31	2019–2022	3 × 182	0.039 (23)	1.5	0.017 (23)	0.3
EC, β^-, β^+	^{152}Eu	SCK	HPGe #32	2020–2022	3 × 105	0.095 (62)	1.2	0.082 (62)	0.9
β^+, EC	^{154}Eu	PTB	IC K	1999–2020	2494	0.0066 (8)	35	0.0018 (8)	2.7
β^+, EC	^{154}Eu	PTB	IC U	2019–2022	415	0.004 (3)	0.7	0.003 (3)	0.3
EC (,β^+)	^{207}Bi	NIST	IC	1971–2011	152	0.031 (9)	6.5	0.011 (9)	0.8
α	^{209}Po	JRC	PIPS	2013–2022	6291	0.0028 (24)	0.7	0.0032 (24)	0.9
$\alpha + \beta^-$	^{226}Ra	JRC	IC	2005–2015	1244	0.0036 (22)	1.3	0.0033 (22)	1.1
$\alpha + \beta^-$	^{226}Ra	BIPM	IC	2001–2022	206	0.0026 (19)	0.9	0.0023 (19)	0.7
$\alpha + \beta^-$	^{226}Ra	NPL	IC	1996–2016	3714	0.0042 (7)	18	0.0018 (7)	3.3
$\alpha + \beta^-$	^{226}Ra	NPL	IC	1997–2016	3746	0.0020 (20)	0.5	0.0011 (20)	0.2
$\alpha + \beta^-$	^{226}Ra	NIST	IC	2012–2016	272	0.001 (7)	0.0	0.002 (7)	0.0
$\alpha + \beta^-$	^{226}Ra	PTB	IC K	1999–2020	1380	0.0113 (15)	28	0.0039 (15)	3.4
$\alpha + \beta^-$	^{226}Ra	PTB	IC U	2019–2022	344	0.004 (3)	0.9	0.004 (3)	0.9
$\alpha + \beta^-$	^{226}Ra	ANSTO	IC	2008–2014	1743	0.004 (19)	0.0	0.010 (19)	0.0
$\alpha + \beta^-$	^{226}Ra	ANSTO	IC	2012–2016	852	0.0050 (29)	1.5	0.0003 (29)	0.0
α	^{228}Th	NIST	IC	1968–1978	70	0.030 (24)	0.8	0.028 (24)	0.7
α	^{230}U	JRC	mix	2011	4731	0.004 (6)	0.2	0.008 (6)	0.9
α	^{241}Am	NPL	IC	2020–2022	521	0.0053 (15)	2.4	0.0010 (15)	0.2
α	^{241}Am	PTB	LSC	2014–2016	574	0.0007 (11)	0.2	0.0004 (11)	0.1

(Continued.)

Table 1. (Continued.)

Decay mode(s)	Nuclide	Institute	Method	Period/year	#Data	Raw data		Humidity-compensated	
						Amplitude A'/%	Power S	Amplitude A'/%	Power S
α	^{241}Am	JSI	HPGe	1198–2014	2852	0.13 (7)	1.6	0.12 (7)	1.2
α	^{241}Am	IAEA	HPGe #12	2018–2023	122	0.14 (9)	1.3	0.01 (9)	0.0
α	^{241}Am	IAEA	HPGe #15	2018–2023	148	0.46 (12)	7.8	0.20 (12)	1.4
α	^{241}Am	IAEA	HPGe 100	2018–2022	167	0.18 (10)	1.8	0.16 (10)	1.4
α	^{241}Am	IAEA	HPGe 170	2018–2022	129	0.06 (16)	0.1	0.10 (16)	0.2
α	^{241}Am	SCK	HPGe #8	2008–2017	500	0.030 (27)	0.6	0.019 (27)	0.3
α	^{241}Am	SCK	HPGe #10	2008–2016	482	0.095 (20)	12	0.037 (20)	1.9
α	^{241}Am	SCK	HPGe #11	2008–2017	487	0.052 (21)	3.0	0.047 (21)	2.4
α	^{241}Am	SCK	HPGe #13	2008–2017	517	0.142 (26)	15	0.051 (26)	2.1
α	^{241}Am	SCK	HPGe #16	2008–2015	409	0.049 (22)	2.4	0.039 (22)	1.6
α	^{241}Am	SCK	HPGe #17	2014–2017	189	0.131 (32)	8.6	0.064 (32)	2.2
α	^{241}Am	SCK	HPGe #20	2013–2019	317	0.149 (50)	4.4	0.152 (50)	4.9
α	^{241}Am	SCK	HPGe #21	2008–2017	412	0.081 (49)	1.4	0.079 (49)	1.2
α	^{241}Am	SCK	HPGe #23	2010–2017	354	0.179 (54)	5.5	0.167 (54)	4.8
α	^{241}Am	SCK	HPGe #24	2011–2017	307	0.017 (16)	0.6	0.016 (16)	0.5
α	^{241}Am	SCK	HPGe #25	2011–2017	326	0.108 (21)	13	0.048 (21)	2.4
α	^{241}Am	SCK	HPGe #26	2013–2017	245	0.018 (22)	0.3	0.017 (22)	0.3
α	^{241}Am	SCK	HPGe #27	2011–2017	305	0.153 (72)	2.3	0.128 (72)	1.6
α	^{241}Am	SCK	HPGe #28	2014–2017	193	0.011 (28)	0.1	0.006 (28)	0.0
α	^{241}Am	SCK	HPGe #8	2019–2022	207	0.148 (55)	3.7	0.134 (55)	3.0
α	^{241}Am	SCK	HPGe #9	2020–2022	121	0.160 (52)	4.8	0.150 (52)	4.3
α	^{241}Am	SCK	HPGe #10	2019–2022	213	0.091 (37)	3.1	0.040 (37)	0.6
α	^{241}Am	SCK	HPGe #11	2019–2022	126	0.019 (53)	0.4	0.015 (53)	0.0
α	^{241}Am	SCK	HPGe #13	2019–2022	217	0.098 (41)	2.9	0.066 (41)	1.3
α	^{241}Am	SCK	HPGe #14	2019–2022	193	0.101 (145)	0.2	0.097 (145)	0.2
α	^{241}Am	SCK	HPGe #19	2019–2022	180	0.126 (42)	4.4	0.059 (42)	1.0
α	^{241}Am	SCK	HPGe #21	2019–2022	182	0.107 (93)	0.7	0.090 (93)	0.5
α	^{241}Am	SCK	HPGe #22	2020–2022	101	0.056 (54)	1.0	0.066 (54)	0.8
α	^{241}Am	SCK	HPGe #23	2019–2020	64	0.072 (81)	0.9	0.073 (81)	0.4
α	^{241}Am	SCK	HPGe #24	2021–2022	84	0.067 (29)	2.3	0.057 (29)	2.0
α	^{241}Am	SCK	HPGe #25	2019–2022	174	0.063 (25)	2.6	0.027 (25)	0.6
α	^{241}Am	SCK	HPGe #26	2019–2022	184	0.085 (36)	2.4	0.040 (36)	0.6
α	^{241}Am	SCK	HPGe #27	2019–2022	171	0.145 (92)	1.6	0.147 (92)	1.3
α	^{241}Am	SCK	HPGe #28	2019–2022	177	0.050 (40)	1.2	0.038 (40)	0.5
α	^{241}Am	SCK	HPGe #30	2019–2022	155	0.070 (22)	3.2	0.063 (22)	4.2
α	^{241}Am	SCK	HPGe #31	2019–2022	182	0.087 (22)	3.9	0.060 (22)	3.8
α	^{241}Am	SCK	HPGe #32	2020–2022	104	0.094 (63)	1.5	0.079 (63)	0.8

[a] Acronyms: LSC liquid scintillation counting; IGC internal gas counting; TDCR triple-to-double coincidence counting ratio; IC ionisation chamber (K Keithley electrometer readout; U ULCA ultrastable low-noise current amplifier); LTAC live-time anti-coincidence counting; HPGe high-purity germanium detector; PPC pressurised proportional counter; PIPS planar Si detector.

Direct evidence of the sensitivity of instruments to environmental factors was collected in the new laboratory wing of the NIST. The behaviour of the 'AutoIC' chamber was continuously monitored by performing source and background measurements while the climate control system generated short-term cyclic variations in temperature and humidity in the laboratory. Figure 4 illustrates how the ionisation current for a ^{223}Ra source in the 'AutoIC' chamber follows the environmental changes with a delay of approximately an hour. This information was persuasive in efforts to prioritise improved climate control as part of the ongoing construction project.

3.3. PTB

Over the years, the PTB has applied three different current measurement methods for their IC (type IG12, 20th Century Electronics, UK); a Townsend balance until 1999, a Keithley electrometer until 2020, and currently an Ultrastable Low-Noise Current Amplifier (ULCA). As a result, the detector has shown different sensitivity to environmental influences. It has already been demonstrated in previous work [8, 59–62] that the Townsend balance appeared to be susceptible to radon concentration in air, which explains the annual cycles

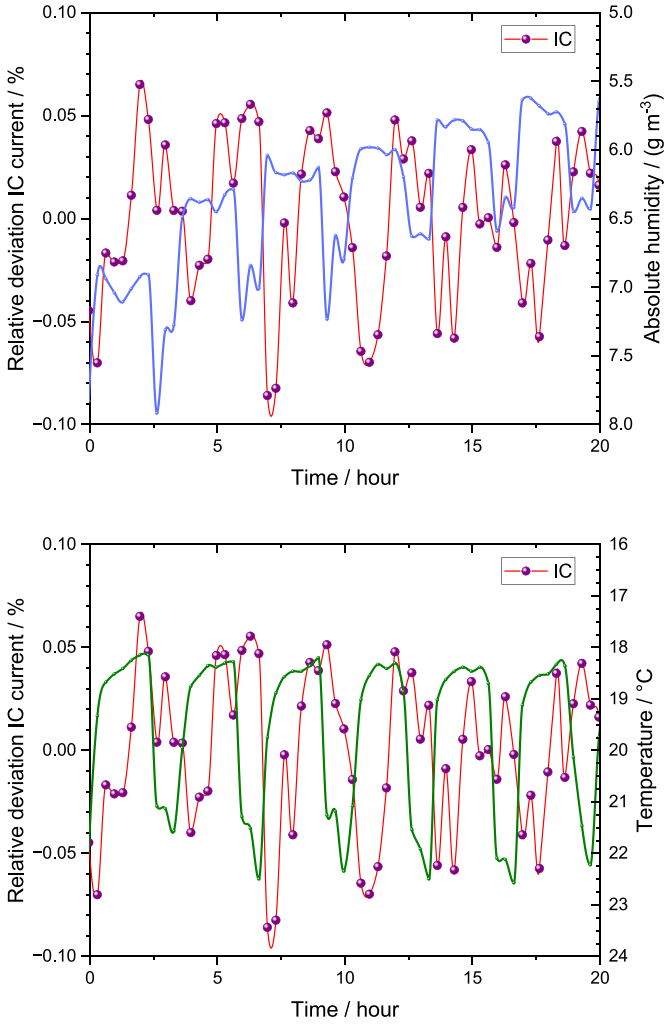

Figure 4. Relative change in ionisation current from a ^{223}Ra source in the 'AutoIC' ionisation chamber at the NIST as a function of time, compared to short-term changes in temperature and absolute humidity in the laboratory generated through the climate control system.

observed in the pre-1999 data sets. These data are not further considered in the paper.

More recent data sets were provided for 11 radionuclides: ^{54}Mn, ^{60}Co, ^{85}Kr, ^{90}Sr, ^{108m}Ag, ^{133}Ba, ^{124}Sb, ^{137}Cs, ^{152}Eu, ^{154}Eu, and ^{226}Ra. Those obtained with the Keithley electrometer generally show some humidity effects, which reduce to an acceptable level after compensation based on humidity data from the Langenhagen weather station. A peculiar case is the beta emitter ^{90}Sr measured in the IC, which manifests a significant annual cycle with power $S = 52$, as shown in figure 5. It would appear that the cycle is synchronised with ambient humidity to a large extent, but there is additional structure due to local instabilities in the data set. There is a gradient in the residuals of -0.0045% per g m^{-3} humidity. Besides that, other influential factors in the measurement conditions may have played a role. As a result, a linear correction proportional with humidity reduces the power of the cycle to $S = 15$, but does not completely cancel the annual trend.

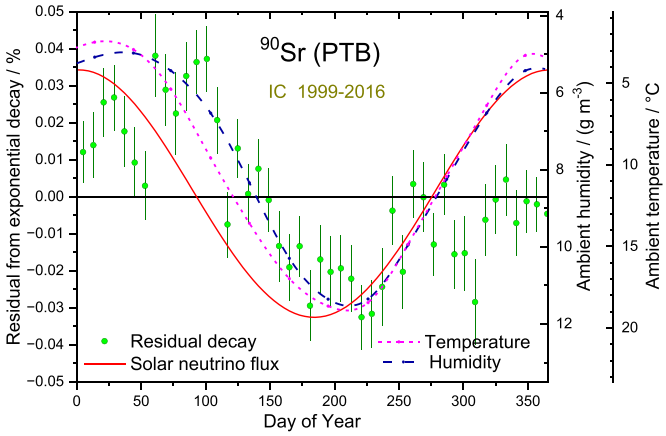

Figure 5. Average residuals from exponential decay for ^{90}Sr decay rates measured at the PTB in an IC, binned over fixed periods in the year. The lines represent the expected relative change in solar neutrino flux hitting Earth (full line), the average ambient temperature (short dash) and humidity (long dash).

The ULCA, developed by PTB [63, 64], has been introduced to measure small currents with low noise and high gain stability. While the 2020–2022 data sets appear to be independent of humidity, there is still some variance present that can be partly attributed to imperfections in geometrical replication of the source positioning using a robot arm. In general, the amplitudes of the fitted annual cycles are statistically insignificant, but reside at the high side of the Rayleigh probability distribution. It should be noted that in order to mitigate the influence of environmental effects in normal praxis, the PTB conducts its calibrations relative to a ^{226}Ra reference source.

The PTB [65, 66] generated particularly stable decay series measurements of ^{36}Cl, ^{90}Sr, and ^{241}Am by means of liquid scintillation counting, applying TDCR in the case of ^{36}Cl and ^{90}Sr and a commercial LSC for ^{241}Am. The data show no correlation with humidity. Undisclosed results of ongoing ^{32}Si decay rate measurements promise exceptional stability, in contrast with the seasonal variations observed in the BNL/Purdue data [67, 68], which were found to be correlated with ambient humidity [17, 18].

3.4. NPL

At the NPL (UK), a long history of ^{226}Ra check source measurements was provided for two well-type re-entrant ICs: a PA782 (2 MPa argon gas, steel inner well) and a Vinten (1 MPa nitrogen gas, 3 mm Al inner well), as well as a more recent series of ^{241}Am measurements in the Vinten IC. Only data obtained since July 1996 could be used in the study, upon the availability of weather information from the Hounslow weather station. The residuals show the presence of a significant annual sinusoidal deviation from exponential decay, which clearly correlates with ambient humidity. Evidence is shown in figure 6. In addition, a series of gamma-ray measurements with lower precision showed a hint of a humidity effect which disappeared after compensation.

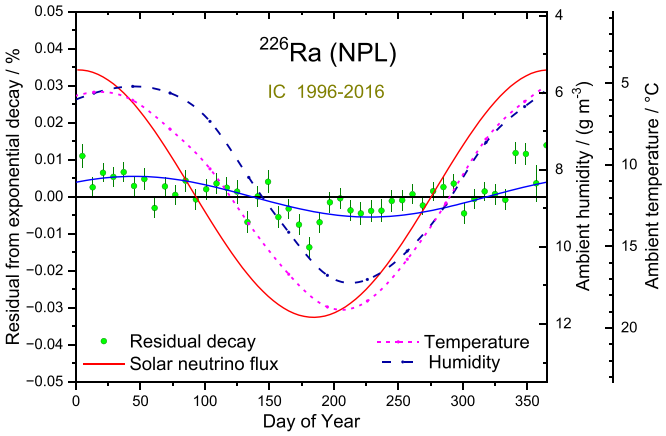

Figure 6. Average residuals from exponential decay for ^{226}Ra decay rates measured in a Vinten IC, binned over fixed periods in the year, and a fitted sinusoidal cycle through the data. The lines represent the expected relative change in solar neutrino flux hitting Earth (full line), the average ambient temperature (short dash) and humidity (long dash) in the Hounslow region.

3.5. BIPM

The BIPM (located in Sèvres) houses the SIR, a system of two Centronics IG11 ICs used as long-term reference instruments by which mono-radionuclide solutions with standardised activities can be compared for international equivalence. The ionisation current is measured with a Keithley electrometer with external capacitors in a sealed box and using the Townsend balance technique. The laboratory room is temperature and humidity controlled. The stability of the IC #389 has been monitored with the ^{226}Ra check source #4 and the residuals from exponential decay between 2001 and 2022 show no annual cycle, and no significant correlation with humidity in the Toussus-le-Noble weather station.

3.6. ANSTO

Additional evidence was collected in the southern hemisphere, at ANSTO (Australia) [8]. Several sets of ^{226}Ra measurements in a TPA Mk-II IC with a Keithley 6517 A electrometer have been combined and turned out to be free of an annual cycle. Records of the response of a medical calibrator (TPA IC with Keithley electrometer) to a ^{226}Ra reference source show also no sign of annual oscillations.

3.7. NMISA

A series of ^{14}C measurements by TDCR in NMISA (South-Africa) showed no significant annual cycle [9].

3.8. IRA

At the IRA (Switzerland), a ^{137}Cs source was measured between 1980 and 2012 in a Centronic IG11 IC and automated readout based on the principle of the Townsend balance. A typical measurement cycle corresponds to the time needed to load a given capacitor up to 0.1 V. Data after 1996 could be compared with humidity values from the Lausanne weather station. There was no notable annual cycle.

3.9. NRC

From NRC (Canada) three small data sets were made available from ^{137}Cs in three different ICs (Capintec, Vinten and TPA). The individual data sets seem correlated with humidity in the Ottawa weather station. In table 1, values are provided for a combination of the data sets.

3.10. ENEA

At the laboratory in Casaccia, thousands of measurements have been performed between 24 March and 12 May 2016 to investigate correlations between the Centronic IG11 IC readouts with a Keithley 617 electrometer for a ^{226}Ra source and various environmental conditions obtained with an AlphaGUARD monitor in the laboratory [8]. The results of the study show a significant correlation ($\rho = 0.84$) between the averaged IC currents and temperature, indicating that temperature variations of several degrees Celsius in the laboratory may be the primary cause of seasonal variations in the IC signals at ENEA. The impact of other environmental conditions, including ambient pressure, relative humidity, and radon concentration in air, was found to be lower ($-0.2 < \rho < 0.2$).

3.11. SCK CEN

In the frame of quality control of the γ-ray spectrometry service at the SCK CEN (Belgium), spectra of mixed ^{152}Eu-^{241}Am reference sources were collected on multiple HPGe spectrometers at a weekly rate. In previous work, data from 2008–2016 were analysed and a strong correlation was found in the annual cycles of characteristic lines of ^{152}Eu and ^{241}Am, however the amplitude of the cycles differed among the detectors [7, 10]. This was considered proof that the instabilities were of instrumental nature and not caused by 'variations in the decay constants due to solar neutrinos'. At that time, the detectors were kept in a temperature-controlled room, without humidity control. Through comparison with climate data from a weather station in Antwerp, evidence suggests that sensitivity of the spectrometers to ambient humidity was the most likely culprit for these seasonal deviations.

In the current work, data sets obtained with 14 HPGe detectors up to Oct 2017 have been (re)analysed. The amplitude of the annual cycle was determined for the peak areas of the 59 keV line of ^{241}Am and for the sum of the 122 keV, 779 keV and 1408 keV peak areas of ^{152}Eu. Weighted mean values for both nuclides are presented in figure 7, showing the amplitude height of the fitted annual cycle as a function of the correlation factor between the decay rates and ambient humidity. The highest annual cycles seem to appear in data sets with

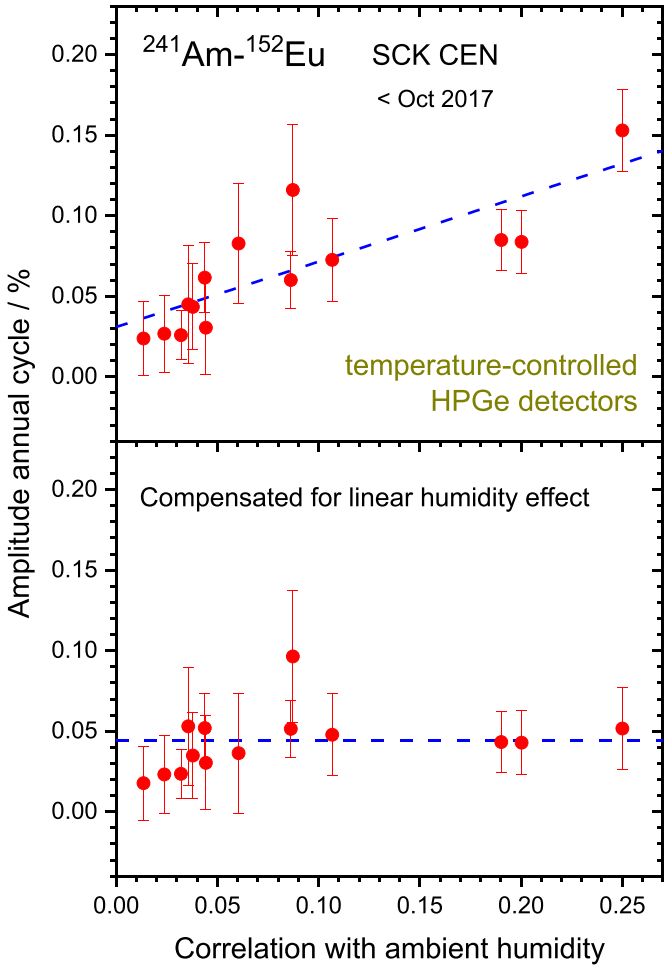

Figure 7. Fitted amplitudes of annual cycles in residuals to exponential decay deduced from one ^{241}Am and three ^{152}Eu peaks in γ-ray spectra of a reference source measured before Oct 2017 with various HPGe detectors in a temperature-controlled laboratory of the SCK CEN in Mol (Belgium). A few detectors show correlation with ambient air humidity causing annual cycles with power up to $S = 10.5$, but no significant cycle persists ($S < 2.2$) after linear compensation based on humidity.

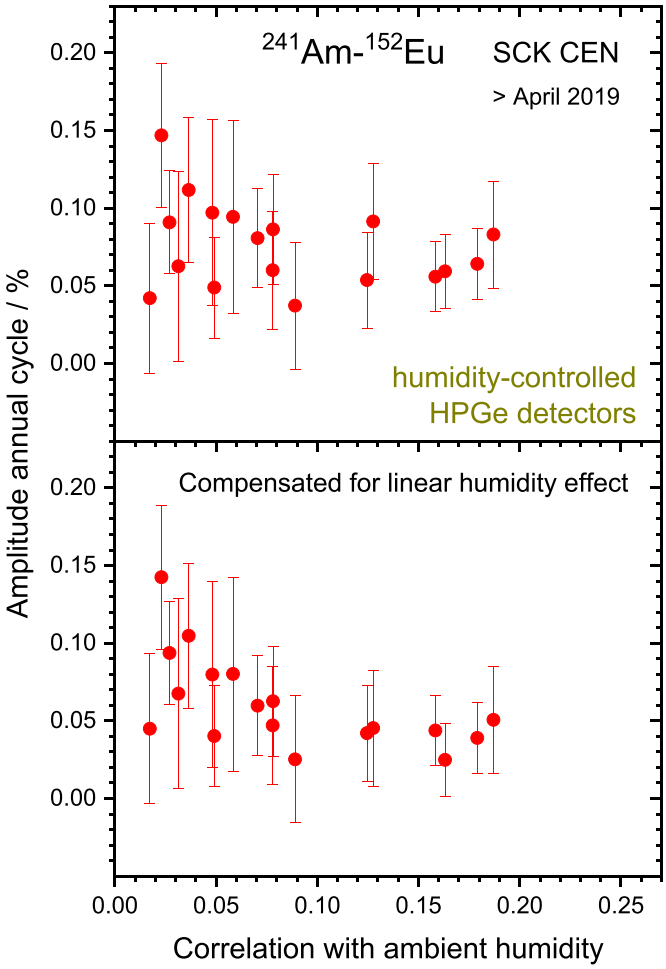

Figure 8. Fitted amplitudes of the annual cycle in residuals to exponential decay deduced from one ^{241}Am and three ^{152}Eu peaks in γ-ray spectra of a mixed reference source measured from Apr 2019 to Dec 2022 with various HPGe detectors in a temperature- and humidity-controlled laboratory of the SCK CEN in Mol (Belgium). No significant annual cycles are found ($S < 2.5$) and compensation for humidity hardly affects the amplitudes ($S < 2.4$).

a relatively high correlation with humidity. Their amplitudes drop to a statistically insignificant level when the individual data are compensated for a hypothesised linear relationship with the average outdoor absolute air humidity at the day of measurement.

By April 2019, the detectors have been moved to a new laboratory equipped with temperature and humidity control. The data sets since that date are less extensive, not necessarily more stable, but show no statistically significant annual cycles. The associated amplitudes remain almost invariant for humidity compensation (figure 8).

3.12. JSI

The JSI (Slovenia) provided quality assurance measurements of ^{60}Co and ^{109}Cd on different HPGe detectors. Results from 5 detectors were combined for ^{60}Co and 3 for ^{109}Cd, and they were compared with weather data from Cerklje. No annual cycle or humidity effect could be identified.

3.13. IAEA

The IAEA environmental laboratory in Monaco conducted quality control measurements of three radionuclides (^{241}Am, ^{137}Cs, ^{60}Co) on four HPGe detectors. Weather data were obtained from the Oceanographic Museum of Monaco and supplemented with data from the airport in Nice. The laboratory room was equipped with a dehumidifier, which effectively suppressed the inside humidity level whenever the ambient humidity exceeded 10 g m^{-3}. Three detectors showed minimal annual cycles, while the measurement results of HPGe #15 exhibited indications of anti-correlation with ambient humidity. For this detector, a mean annual cycle of 0.33 (7)% amplitude was observed, which reduced to 0.17 (7)% after compensating for humidity.

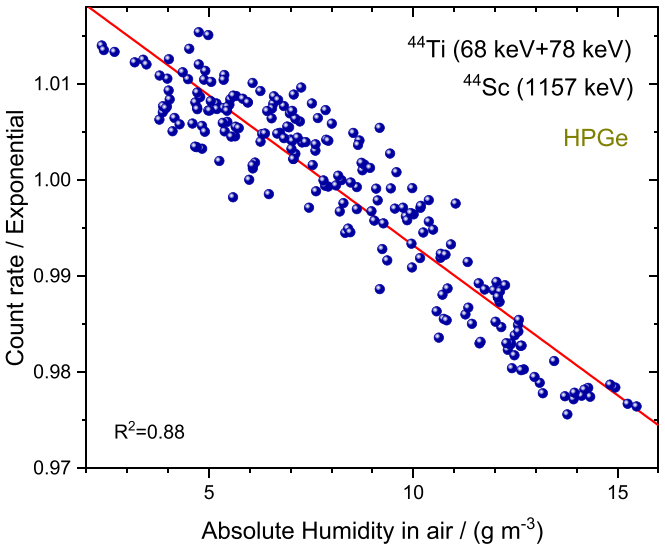

Figure 9. Correlation plot between a moving average of the absolute ambient humidity, as measured in a weather station at the PSI, and relative departures from exponential decay of the count rates in the γ-ray peaks at 68 keV and 78 keV from ^{44}Ti decay, and at 1157 keV from ^{44}Sc decay.

3.14. PSI

The PSI reported severe instabilities in the percent range in decay rate series of ^{171}Tm, ^{145}Sm, and ^{44}Ti measured on a HPGe detector with imperfect vacuum in the crystal housing [69, 70]. It was found that the variations in the count rates over the measurement campaign were highly correlated with the absolute humidity outside the laboratory. A correlation plot is shown in figure 9. The count rate variations went hand in hand with shifts in the energy calibration.

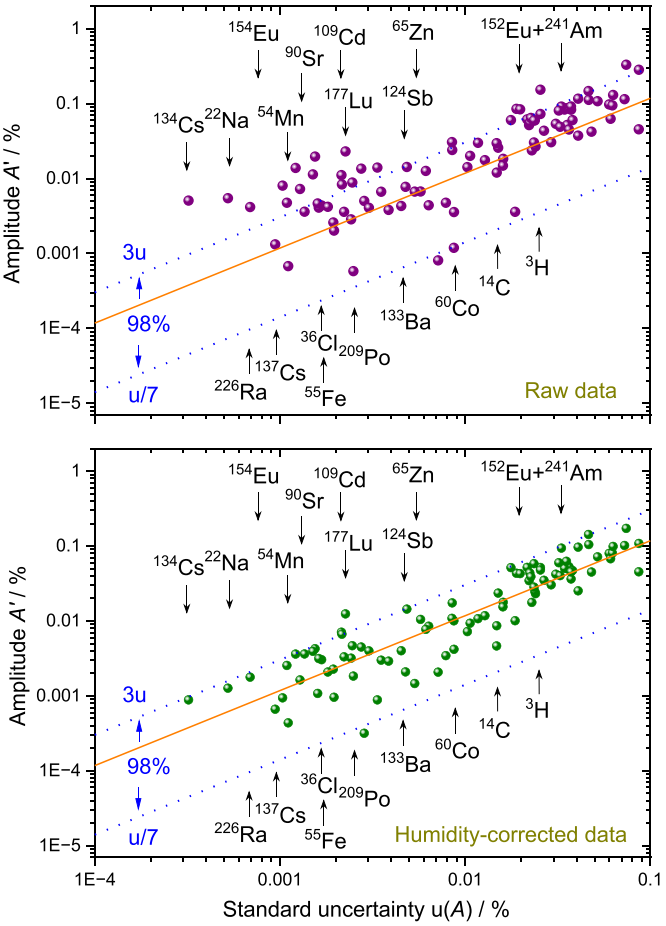

Figure 10. Amplitude of annual cycles in residuals to exponential decay as a function of their standard uncertainty, before (top) and after (bottom) a humidity correction. The solid line shows the expected median amplitude of noise data, and the dotted lines indicate the statistical boundaries where only 1% of noise data would cross either line.

4. Discussion

Table 1 summarises the amplitudes and powers of the fitted annual cycles to the residuals from exponential decay, before and after compensation for a humidity effect. Figure 10 illustrates the relationship between the amplitudes and their standard uncertainties. The lines in the graph represent the expected region in which the annual cycles in random noise data would appear, following a Rayleigh distribution. The findings indicate that several decay rate series generated a statistically significant annual cycle above the noise band. However, after compensating for a linear relationship with ambient humidity, the annual cycle in almost every data set decreased to a statistically insignificant value. While this may not provide conclusive evidence that ambient humidity was the underlying cause for the instability in all these measurements, it is a likely factor in many.

These results are remarkable given the crude compensation for humidity in the laboratory at the time of measurement. Meteorological data from a weather station located several kilometres away from the laboratories were used, and daily averaged values were employed instead of more precise values as a function of time. Additionally, the method did not account for specific conditions in the laboratory induced by (sometimes failing) heating and climate systems, and differences between day and night regimes, weekdays and weekends or holiday periods. A more rigorous treatment of the data would require characterisation of each measurement system for the response change as a function of environmental conditions as well as monitoring of those conditions during half-life determinations. Although that data was not available for this extensive dataset, the proxy data make a strong case that the studies to account for humidity effects are necessary and humidity effects must be excluded before more exotic explanations are considered reasonable.

Humidity can have a significant influence on IC measurements. On a hypothetical level, it can alter the dielectric properties of the medium surrounding the IC, which could affect the electric field within the chamber and thus influence the collection of ionisation charges. More importantly, humidity can affect the stability of the electronic components in the electrometer or voltmeter used to measure the ionisation current or voltage across a capacitor [71]. Moreover, it can increase the conductivity of air, leading to enhanced discharge of an

external air capacitor over which the ionisation current is collected. This can lead to a change in the voltage measured across the capacitor for a given ionisation current. The air capacitor can also be discharged by radon and progeny alpha decays in air, so it is good practice to keep it shielded from environmental influences and ionising radiation, including the source in the IC. The IC can be shielded with materials such as lead to reduce the amount of external radiation (incl. secondary cosmic radiation) that reaches the chamber.

High-purity germanium (HPGe) detectors for gamma-ray spectrometry are very sensitive instruments that require a stable operating environment. Ambient humidity can impact the performance of HPGe detectors, particularly if the vacuum inside the crystal housing is not well-maintained. When the vacuum is inadequate, moisture in the air can enter the crystal housing and condense on the surface of the HPGe detector crystal. This moisture can create a thin film on the crystal's surface, which can act as an electrical conductor, thereby increasing the leakage current of the detector. This increase in leakage current can lead to higher baseline noise levels in the spectra, reducing the sensitivity and resolution of the detector. Furthermore, the condensed water can create additional electrical noise due to the formation of a capacitive circuit between the crystal and the grounding circuit, which can lead to spikes in the spectra. These spikes can make it more difficult to identify and quantify peaks in the gamma-ray spectrum.

Some techniques, e.g. liquid scintillation counting, alpha-particle counting with planar Si detectors, show no significant dependency on ambient humidity. The measurements discussed in this paper mostly refer to decay rates of the order of kBq, which are not highly sensitive to changes in the background event rate. Low-level activity measurements are more susceptible to various natural processes, such as radon emanation and cosmic muons interacting with Earth's atmosphere.

5. Conclusions

The influence of ambient humidity on radiation detectors has been investigated in numerous decay rate measurement series from 14 laboratories. Several data sets displayed annual cycles at various levels of statistical significance. For each data set, a linear relationship was derived from a correlation plot between the residuals from exponential decay and the average daily ambient humidity values from nearby weather stations. The corresponding offset and slope were used to compensate the residuals in the activity measurements for the assumed humidity effect. As a result, the annual cycles dropped to a statistically insignificant level in virtually all tested decay series and the validity of the exponential-decay law could be confirmed with an accuracy on the amplitude ranging from 0.0003% to 0.1%. The present analysis demonstrates that annual cycles observed in radioactivity measurements may be attributed to environmental factors such as humidity and temperature variations that affect the performance of the measurement equipment. It leaves less room for alternative theories such as the hypothesis of solar neutrinos influencing the radioactive decay process itself. Radionuclide metrology can gain additional confidence in measurements by characterising the sensitivity of measurement systems to environmental conditions and by monitoring and controlling those conditions that have a significant impact.

6. Disclaimer

Certain commercial equipment, instruments, or materials are identified in this report to foster understanding. Such identification does not imply recommendation by the authors' institutes, nor does it imply that the materials or equipment identified are necessarily the best available for the purpose.

Acknowledgments

This work has been presented at the 23rd International Conference on Radionuclide Metrology and its Applications in Bucharest, Romania in 2023.

ORCID iDs

S Pommé https://orcid.org/0000-0001-5017-7451
D E Bergeron https://orcid.org/0000-0003-1150-7950
R Coulon https://orcid.org/0000-0001-9851-0890
K Pelczar https://orcid.org/0000-0001-9504-1750

References

[1] Pommé S 2022 Radionuclide metrology—confidence in radioactivity measurements *JRC Technical Report, EUR 31134 EN* (European Commission) JRC129308 (https://doi.org/10.2760/666973)
[2] Pommé S 2022 Radionuclide metrology—confidence in radioactivity measurements *J. Radioanal. Nucl. Chem.* **331** 4771
[3] Pommé S 2016 When the model doesn't cover reality: examples from radionuclide metrology *Metrologia* **53** S55
[4] Pommé S and Pelczar K 2022 Neutrino-induced decay: a critical review of the arguments *Space Sci. Rev.* **218** 64
[5] McDuffie M H *et al* 2020 Anomalies in radioactive decay rates: a bibliography of measurements and theory (arXiv:2012.00153)
[6] Sturrock P A 2022 Neutrino-flux variability, nuclear-decay variability, and their apparent relationship *Space Sci. Rev.* **218** 23
[7] Pommé S *et al* 2016 Evidence against solar influence on nuclear decay constants *Phys. Lett.* B **761** 281
[8] Pommé S *et al* 2017 On decay constants and orbital distance to the Sun—part I: alpha decay *Metrologia* **54** 1
[9] Pommé S *et al* 2017 On decay constants and orbital distance to the Sun—part II: beta minus decay *Metrologia* **54** 19
[10] Pommé S *et al* 2017 On decay constants and orbital distance to the Sun—part III: beta plus and electron capture decay *Metrologia* **54** 36
[11] Pommé S, Kossert K and Nähle O 2017 On the claim of modulations in ^{36}Cl beta decay and their association with solar rotation *Solar Phys.* **292** 162
[12] Pommé S *et al* 2018 Is decay constant? *Appl. Radiat. Isot.* **134** 6
[13] Pommé S, Lutter G, Marouli M, Kossert K and Nähle O 2018 On the claim of modulations in radon decay and their association with solar rotation *Astropart. Phys.* **97** 38

[14] Pommé S, Lutter G, Marouli M, Kossert K and Nähle O 2019 A reply to the rebuttal by Sturrock et al *Astropart. Phys.* **107** 22

[15] Pommé S 2019 Solar influence on radon decay rates: irradiance or neutrinos? *Eur. Phys. J.* C **79** 73

[16] Pommé S and Pelczar K 2020 On the recent claim of correlation between radioactive decay rates and space weather *Eur. Phys. J.* C **80** 1093

[17] Pommé S, Pelczar K, Kossert K and Kajan I 2021 On the interpretation of annual oscillations in ^{32}Si and ^{36}Cl decay rate measurements *Sci. Rep.* **11** 16002

[18] Pommé S and Pelczar K 2022 Role of ambient humidity underestimated in research on correlation between radioactive decay rates and space weather *Sci. Rep.* **12** 2527

[19] Pommé S, Pelczar K and Kajan I 2022 Air humidity and annual oscillations in ^{90}Sr/^{90}Y and ^{60}Co decay rate measurements *Sci. Rep.* **12** 9535

[20] Pommé S 2015 Typical uncertainties in alpha-particle spectrometry *Metrologia* **52** S146

[21] Lépy M-C, Pierce A and Sima O 2015 Uncertainties in gamma-ray spectrometry *Metrologia* **52** S123

[22] Pommé S 2007 Methods for primary standardization of activity *Metrologia* **44** S17

[23] Pommé S, Fitzgerald R and Keightley J 2015 Uncertainty of nuclear counting *Metrologia* **52** S3

[24] Pommé S 2015 The uncertainty of counting at a defined solid angle *Metrologia* **52** S73

[25] Fitzgerald R, Bailat C, Bobin C and Keightley J D 2015 Uncertainties in 4πβ–γ coincidence counting *Metrologia* **52** S86

[26] Thiam C, Bobin C, Maringer F J, Peyres V and Pommé S 2015 Assessment of the uncertainty budget associated with 4πγ counting *Metrologia* **52** S97

[27] Unterweger M, Johansson L, Karam L, Rodrigues M and Yunoki A 2015 Uncertainties in internal gas counting *Metrologia* **52** S156

[28] Kossert K, Broda R, Cassette P, Ratel G and Zimmerman B 2015 *Metrologia* **52** S172

[29] Johansson L, Altzitzoglou T, Sibbens G, Pommé S and Denecke B 2003 Standardisation of ^{238}Pu using four methods of measurement *Nucl. Instrum. Methods Phys. Res* A **505** 699

[30] Pommé S, Altzitzoglou T, Van Ammel R and Sibbens G 2005 Standardisation of ^{125}I using seven techniques for radioactivity measurement *Nucl. Instrum. Methods Phys. Res.* A **544** 584

[31] Pommé S, Altzitzoglou T, Van Ammel R and Sibbens G 2021 Standardisation of ^{241}Am activity for a key comparison *J. Radioanal. Nucl. Chem.* **330** 985

[32] Pommé S 2015 The uncertainty of the half-life *Metrologia* **52** S51

[33] Pommé S, Stroh H and Benedik L 2015 Confirmation of 20% error in the ^{209}Po half-life *Appl. Radiat. Isot.* **97** 84

[34] Pommé S and Benedik L 2016 On the ^{209}Po half-life error and its confirmation: an answer to the critique *J. Radioanal. Nucl. Chem.* **309** 931

[35] Pommé S, Paepen J and Van Ammel R 2018 Linearity check of an ionisation chamber through ^{99m}Tc half-life measurements *Appl. Radiat. Isot.* **140** 171

[36] Pommé S 2007 Problems with the uncertainty budget of half-life measurements *Applied Modeling and Computations in Nuclear Science* (*ACS Symposium Series* vol 945) ed T M Semkow, S Pommé, S M Jerome and D J Strom (American Chemical Society) p 282

[37] Pommé S, Camps J, Van Ammel R and Paepen J 2008 Protocol for uncertainty assessment of half-lives *J. Radioanal. Nucl. Chem.* **276** 335

[38] Pommé S and Pelczar K 2021 Empirical decomposition and error propagation of medium-term instabilities in half-life determinations *Metrologia* **58** 035012

[39] Pommé S and De Hauwere T 2020 On the significance of modulations in time series *Nucl. Instrum. Methods Phys. Res.* A **956** 163377

[40] Mander P 2012 Formula for calculating absolute humidity (available at: https://carnotcycle.wordpress.com/2012/08/04/how-to-convert-relative-humidity-to-absolute-humidity/)

[41] Bolton D 1980 The computation of equivalent potential temperature *Mon. Weather Rev.* **108** 1046

[42] Huang J 2018 A simple accurate formula for calculating saturation vapor pressure of water and ice *J. Appl. Meteorol. Climatol.* **57** 1265

[43] WMO (World Meteorological Organization) 2021 Guide to instruments and methods of observation: volume I—measurement of meteorological variables WMO-No. 8

[44] Mander P 2017 Formula for computing dew point temperature T_D (available at: https://carnotcycle.wordpress.com/2017/08/01/compute-dewpoint-temperature-from-rh-t/)

[45] Weather Underground, 2023. Antwerp International Airport Station, Antwerp, Belgium, weather history (available at: www.wunderground.com/history/monthly/be/antwerp/EBAW/date/2023–1)

[46] Pommé S, Stroh H and Paepen J 2023 Measurement of the ^{22}Na half-life and evidence supporting the exponential-decay law *Nucl. Data Sheets* accepted

[47] Pommé S, Stroh H and Paepen J 2023 Measurement of the ^{134}Cs half-life in support of the exponential-decay law *Nucl. Data Sheets* submitted

[48] Pommé S 2020 Comparing significance criteria for cyclic modulations in time series *Nucl. Instrum. Methods Phys. Res.* A **968** 163933

[49] Van Ammel T, Pommé S and Sibbens G 2004 Experimental verification of the half-life of ^{65}Zn *Appl. Radiat. Isot.* **60** 337

[50] Van Ammel R, Paepen J, Pommé S and Sibbens G 2010 Measurement of the ^{54}Mn half-life *Appl. Radiat. Isot.* **68** 2387

[51] Paepen J, Altzitzoglou T, Van Ammel R, Sibbens G and Pommé S 2010 Half-life measurement of ^{124}Sb *Appl. Radiat. Isot.* **68** 1555

[52] Van Ammel R, Pommé S, Paepen J and Sibbens G 2011 Measurement of the ^{109}Cd half-life *Appl. Radiat. Isot.* **69** 785

[53] Pommé S, Paepen J, Altzitzoglou T, Van Ammel R and Yeltepe E 2011 Measurement of the ^{177}Lu half-life *Appl. Radiat. Isot.* **69** 1267

[54] Van Ammel T, Pommé S and Sibbens G 2006 Half-life measurement of ^{55}Fe *Appl. Radiat. Isot.* **64** 1412

[55] Pommé S, Stroh H and Van Ammel R 2019 The ^{55}Fe half-life measured with a pressurised proportional counter *Appl. Radiat. Isot.* **148** 27

[56] Pommé S *et al* 2012 Measurement of the ^{230}U half-life *Appl. Radiat. Isot.* **70** 1900

[57] Fitzgerald R 2012 NIST ionization chamber 'A' sample-height corrections *J. Res. Natl Inst. Stand. Technol.* **117** 80

[58] Unterweger M and Fitzgerald R 2020 Corrigendum to 'Update of NIST half-life results corrected for ionization chamber source-holder instability' [Appl. Radiat. Isot. 87 (2014) 92-94] *Appl. Radiat. Isot.* **159** 108976

[59] Siegert H, Schrader H and Schötzig U 1998 Half-life measurements of europium radionuclides and the long-term stability of detectors *Appl. Radiat. Isot.* **49** 1397

[60] Schrader H 2010 Half-life measurements of long-lived radionuclides—new data analysis and systematic effects *Appl. Radiat. Isot.* **68** 1583

[61] Schrader H 2016 Seasonal variations of decay rate measurement data and their interpretation *Appl. Radiat. Isot.* **114** 202
[62] Nähle O and Kossert K 2015 Comment on 'Comparative study of beta-decay data for eight nuclides measured at the Physikalisch-Technische Bundesanstalt' [Astropart Phys 59 (2014) 8–10] *Astropart. Phys.* **66** 8
[63] Drung D, Götz M, Pesel E and Scherer H 2015 Improving the traceable measurement and generation of small direct currents *IEEE Trans. Instrum. Meas.* **64** 3021
[64] Drung D, Krause C, Becker U, Scherer H and Ahlers F J 2015 Ultrastable low-noise current amplifier: a novel device for measuring small electric currents with high accuracy *Rev. Sci. Instrum.* **86** 024703
[65] Kossert K and Nähle O 2014 Long-term measurements of ^{36}Cl to investigate potential solar influence on the decay rate *Astropart. Phys.* **55** 33
[66] Kossert K and Nähle O 2015 Disproof of solar influence on the decay rates of ^{90}Sr/^{90}Y *Astropart. Phys.* **69** 18
[67] Alburger D E, Harbottle G and Norton E F 1986 Half-life of ^{32}Si *Earth Planet. Sci. Lett.* **78** 168
[68] Heim J 2015 The determination of the half-life of Si-32 and time varying nuclear decay Purdue e-Pubs *Open Access Dissertations 1415* (available at: https://docs.lib.purdue.edu/open_access_dissertations/1415)
[69] Kajan I, Pommé S, Pelczar K and Heinitz S 2021 Measurement of the ^{145}Sm half-life *Appl. Radiat. Isot.* **178** 109978
[70] Kajan I, Pommé S and Heinitz S 2022 Measurement of the ^{171}Tm half-life *J. Radioanal. Nucl.* **331** 645
[71] Teverovsky A 2003 Effect of moisture on characteristics of surface mount solid tantalum capacitors *Proc 23rd Capacitor Resistor Technol. Symp.* p 96